Transverse-momentum and pseudorapidity distributions of charged hadrons in pp collisions at $\sqrt{s} = 0.9$ and 2.36 TeV

C. Roland for the CMS Collaboration
Massachusetts Institute of Technology, Cambridge, MA, USA

Measurements of inclusive charged-hadron transverse-momentum and pseudorapidity distributions are presented for proton-proton collisions at $\sqrt{s} = 0.9$ and 2.36 TeV. The data were collected with the CMS detector during the LHC commissioning in December 2009. For non-single-diffractive interactions, the average charged-hadron transverse momentum is measured to be 0.46 ± 0.01 (stat.) $\pm$ 0.01 (syst.) GeV/c at 0.9 TeV and 0.50 ± 0.01 (stat.) $\pm$ 0.01 (syst.) GeV/c at 2.36 TeV, for pseudorapidities between -2.4 and $+2.4$. At these energies, the measured pseudorapidity densities in the central region, $dN_{\rm ch}/d\eta|_{|\eta|<0.5}$, are 3.48 ± 0.02 (stat.) $\pm$ 0.13 (syst.) and 4.47 ± 0.04 (stat.) $\pm$ 0.16 (syst.), respectively. The results at 0.9 TeV are in agreement with previous measurements and confirm the expectation of near equal hadron production in $\rm p\bar{p}$ and pp collisions.

1 Introduction

Measurements of transverse-momentum ($p_{\rm T}$) and pseudorapidity (η) distributions are reported for charged hadrons produced in proton-proton (pp) collisions at centre-of-mass energies ($\sqrt{s}$) of 0.9 and 2.36 TeV at the CERN Large Hadron Collider (LHC) [1]. The data were recorded with the Compact Muon Solenoid (CMS) experiment in December 2009 during two 2-hour periods of the LHC commissioning.

The bulk of the particles produced in pp collisions arises from soft interactions, which are only modeled phenomenologically. Therefore experimental results have to provide guidance for the tuning of these widely-used models and event generators. Soft collisions are usually divided into several categories, namely elastic scattering, inelastic single-diffractive (SD) and double-diffractive (DD) dissociation (Double Pomeron Exchange is treated as DD in this paper), and inelastic non-diffractive (ND) scattering [3]. The distributions shown in this paper are measured for inelastic non-single-diffractive (NSD) interactions to minimize the model dependence of the necessary corrections for the event selection, and to enable a comparison with earlier experiments.

2 Experimental Methods

A detailed description of the CMS experiment can be found in Ref. [2]. The detectors used for the present analysis are the pixel and silicon-strip tracker (SST) covering the η range to $|\eta| < 2.5$, embedded in a 3.8 T magnetic field. The pixel tracker consists of three barrel layers and two end-cap disks at each barrel end. The forward calorimeter (HF), which covers the region $2.9 < |\eta| < 5.2$, was used for event selection. The detailed Monte Carlo simulation (MC) of the CMS detector response is based on GEANT4 [4].

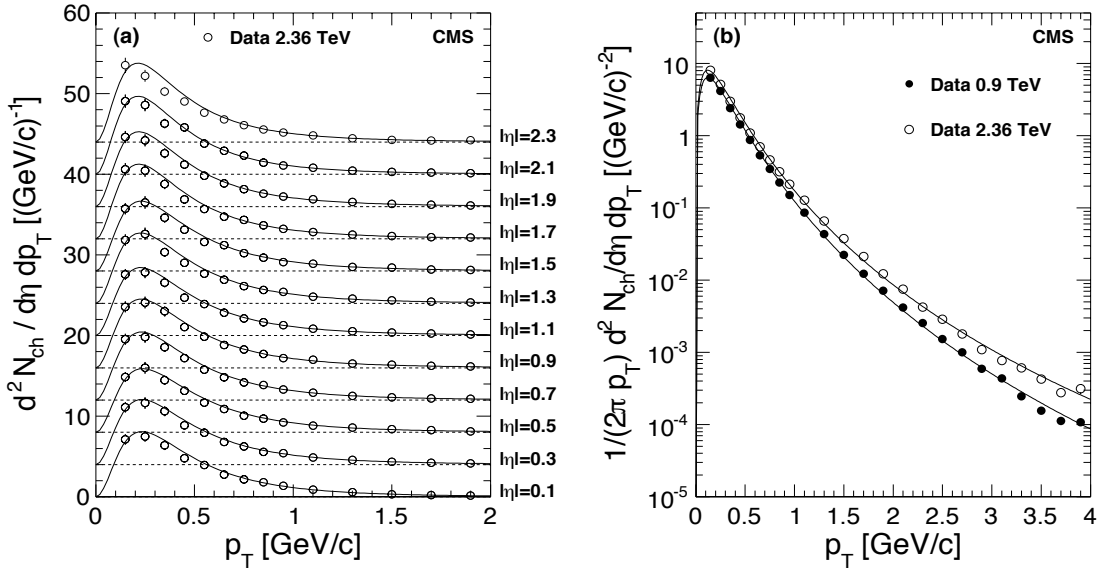

Figure 1: (a) Measured differential yield of charged hadrons in the range $|\eta| < 2.4$ in 0.2-unit-wide bins of $|\eta|$ for the 2.36 TeV data. The measured values with systematic uncertainties (symbols) and the fit functions (Eq. 1) are displayed. The values with increasing η are successively shifted by four units along the vertical axis. (b) Measured yields of charged hadrons for $|\eta| < 2.4$ with systematic uncertainties (symbols), fit with the empirical function (Eq. 1).

For the purpose of this analysis, predominantly NSD events were selected by requiring a primary vertex (PV) to be reconstructed with the tracker, together with at least one HF tower with more than 3 GeV total energy on each side. The event selection efficiency was estimated with simulated events using the PYTHIA[6] and PHOJET[7,8] event generators. The measurements were corrected for the selection efficiency of NSD processes and for the fraction of SD events contained in the data sample after the event selection.

The $dN_{\rm ch}/d\eta$ distributions were obtained with three methods based on counting (i) reconstructed clusters in the barrel part of the pixel detector; (ii) pixel tracklets composed of pairs of clusters in different pixel barrel layers; and (iii) tracks reconstructed in the full tracker volume. The latter method also allows a measurement of the $dN_{\rm ch}/dp_{\rm T}$ distribution. The three methods are sensitive to particles down to $p_{\rm T}$ values of about 30, 50 and 100 MeV/c, respectively, and a correction was applied to the final results of the three methods to extrapolate to $p_{\rm T} = 0$. The measurements were corrected for the geometrical acceptance, efficiency, fake and duplicate tracks, low-$p_{\rm T}$ particles curling in the axial magnetic field, decay products of long-lived hadrons, photon conversions and inelastic hadronic interactions in the detector material. A more detailed description of the event selection and analysis methods can be found in Ref.[5].

3 Results

The $dN_{\rm ch}/dp_{\rm T}$ distributions of charged particles were measured in 12 different η bins, within $|\eta| < 2.4$. The average charged-hadron yields in NSD events are shown in Fig. 1(a), as a function of $p_{\rm T}$ and $|\eta|$. The Tsallis parametrization[9,10]:

$$E\frac{d^3N_{\rm ch}}{dp^3} = \frac{1}{2\pi p_T}\frac{E}{p}\frac{d^2N_{\rm ch}}{d\eta dp_T} = C\frac{dN_{\rm ch}}{dy}\left(1+\frac{E_T}{nT}\right)^{-n} \quad (1)$$

was fit to the data. The $p_{\rm T}$ spectrum of charged hadrons, $1/(2\pi p_{\rm T})d^2N_{\rm ch}/d\eta dp_{\rm T}$, measured in the range $|\eta| < 2.4$ is shown in Fig. 1(b). The fit to the data (Eq. 1) is mainly used for

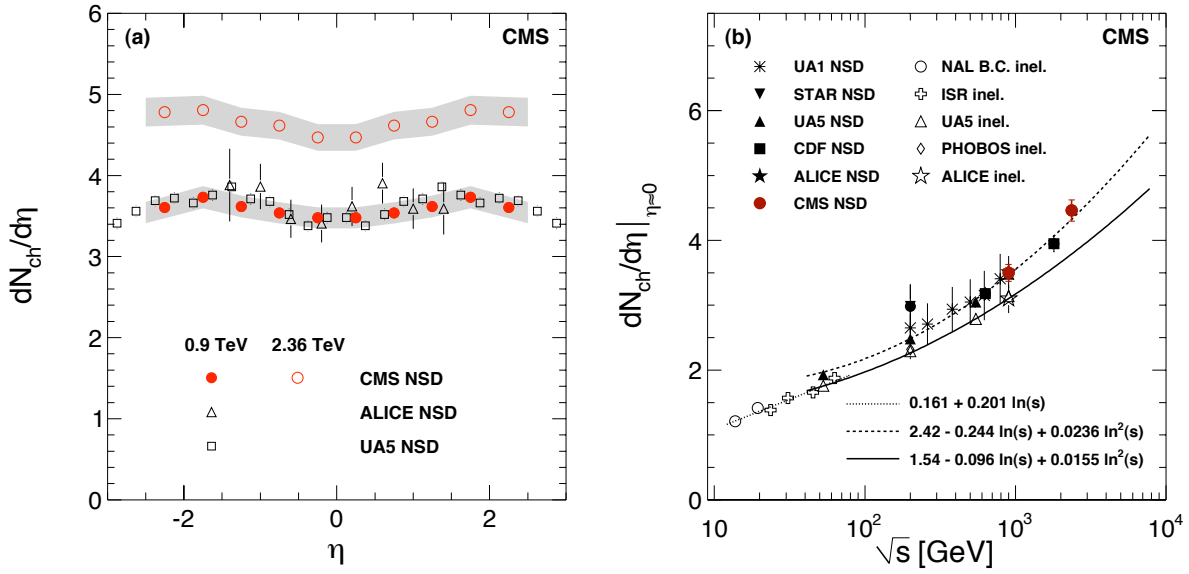

Figure 2: (a) Reconstructed $dN_{\rm ch}/d\eta$ distributions averaged over the cluster counting, tracklet and tracking methods (circles), compared to data from the UA5 (open squares) and from the ALICE (open triangles) experiments at 0.9 TeV, and the averaged result over the three methods at 2.36 TeV (open circles). The CMS and UA5 data points are symmetrized in η. The shaded band represents systematic uncertainties of this measurement, which are largely correlated point-to-point. The error bars on the UA5 and ALICE data points are statistical only. (b) Charged-hadron pseudorapidity density in the central region as a function of centre-of-mass energy in pp and p$\bar{\rm p}$ collisions including lower energy data, together with various empirical parameterizations fit to the data corresponding to the inelastic (solid and dotted curves with open symbols) and to the NSD (dashed curve with solid symbols) event selection. The error bars indicate systematic uncertainties, when available.

extrapolations to $p_{\rm T}$=0, but is not expected to give a perfect description of the data in all η bins with only two parameters. For the 0.9 TeV data, the inverse slope parameter and the exponent were found to be $T = 0.13 \pm 0.01$ GeV and $n = 7.7 \pm 0.2$. For the 2.36 TeV data, the values were $T = 0.14 \pm 0.01$ GeV and $n = 6.7 \pm 0.2$. The average transverse momentum, calculated from the measured data points adding the low- and high-$p_{\rm T}$ extrapolations from the fit is $\langle p_{\rm T} \rangle = 0.46 \pm 0.01$ (stat.) $\pm$ 0.01 (syst.) GeV/c for the 0.9 TeV and 0.50 ± 0.01 (stat.) $\pm$ 0.01 (syst.) GeV/c for the 2.36 TeV data. The summary of results on the pseudorapidity density distribution of charged hadrons is shown in Fig. 2. The results from the three different analysis methods are in agreement and are combined to form the final measurement. The resulting $dN_{\rm ch}/d\eta$ distributions are shown in Fig. 2a for $\sqrt{s}$ = 0.9 and 2.36 TeV and are compared to measurements by other experiments. The shaded error band on the CMS data indicates systematic uncertainties, while the error bars on the data from UA5 [14] and ALICE [16] display statistical uncertainties only. For $|\eta| < 0.5$, the corrected results average to $dN_{\rm ch}/d\eta = 3.48 \pm 0.02$ (stat.) $\pm$ 0.13 (syst.) and $dN_{\rm ch}/d\eta = 4.47 \pm 0.04$ (stat.) $\pm$ 0.16 (syst.) for NSD events at $\sqrt{s}$ = 0.9 and 2.36 TeV. The collision energy dependence of the measured $dN_{\rm ch}/d\eta|_{\eta \approx 0}$ is shown in Fig. 2b, which includes data from the NAL Bubble Chamber [12], the ISR [13], and UA1 [11], UA5 [14], CDF [15], STAR [17], PHOBOS [18] and ALICE [16]. The $dN_{\rm ch}/d\eta$ measurement reported here is consistent with the previously observed trend.

4 Summary

Inclusive measurements of charged-hadron densities, $dN_{\rm ch}/dp_{\rm T}$ and $dN_{\rm ch}/d\eta$, have been presented based on the first pp collisions recorded at $\sqrt{s}$ = 0.9 and 2.36 TeV by the CMS experiment.

For NSD interactions, the average charged-hadron transverse momentum has been measured to be 0.46 ± 0.01 (stat.) $\pm$ 0.01 (syst.) GeV/c at 0.9 TeV and 0.50 ± 0.01 (stat.) $\pm$ 0.01 (syst.) GeV/c at 2.36 TeV. The pseudorapidity density in the central region, $dN_{\rm ch}/d\eta|_{|\eta|<0.5}$, has been measured to be 3.48 ± 0.02 (stat.) $\pm$ 0.13 (syst.) at 0.9 TeV and 4.47 ± 0.04 (stat.) $\pm$ 0.16 (syst.) at 2.36 TeV. The results at 0.9 TeV have been found to be in agreement with previous measurements in $\rm p\bar{p}$ and pp collisions. The increase of $(28.4 \pm 1.4 \pm 2.6)\%$ from 0.9 to 2.36 TeV is significantly larger than the 18.5% (14.5%) increase predicted by the PYTHIA (PHOJET) model tunes used in this analysis.

Acknowledgments

We congratulate and express our gratitude to our colleagues in the CERN accelerator departments for the excellent performance of the LHC. We thank the technical and administrative staff at CERN and other CMS institutes, and acknowledge support from: FMSR (Austria); FNRS and FWO (Belgium); CNPq, CAPES, FAPERJ, and FAPESP (Brazil); MES (Bulgaria); CERN; CAS, MoST, and NSFC (China); COLCIENCIAS (Colombia); MSES (Croatia); RPF (Cyprus); Academy of Sciences and NICPB (Estonia); Academy of Finland, ME, and HIP (Finland); CEA and CNRS/IN2P3 (France); BMBF, DFG, and HGF (Germany); GSRT (Greece); OTKA and NKTH (Hungary); DAE and DST (India); IPM (Iran); SFI (Ireland); INFN (Italy); NRF and WCU (Korea); LAS (Lithuania); CINVESTAV, CONACYT, SEP, and UASLP-FAI (Mexico); PAEC (Pakistan); SCSR (Poland); FCT (Portugal); JINR (Armenia, Belarus, Georgia, Ukraine, Uzbekistan); MST and MAE (Russia); MSTDS (Serbia); MICINN and CPAN (Spain); Swiss Funding Agencies (Switzerland); NSC (Taipei); TUBITAK and TAEK (Turkey); STFC (United Kingdom); DOE and NSF (USA).

References

1. L. Evans, (ed.) and P. Bryant, (ed.), *JINST* **3** (2008) S08001.
2. **CMS** Collaboration, "The CMS experiment at the CERN LHC," S. Chatrchyan et al., *JINST* **3** (2008) S08004.
3. W. Kittel and E. A. De Wolf, "Soft Multihadron Dynamics". (World Scientific, Singapore, 2005).
4. **Geant4** Collaboration, S. Agostinelli et al., *Nucl. Instrum. and Methods* **A506** (2003) 250.
5. **CMS** Collaboration, V. Khachatryan et al., JHEP **1002**, (2010) 041.
6. T. Sjöstrand, S. Mrenna, and P. Skands, "PYTHIA 6.4 Physics and Manual; v6.420, tune D6T," *JHEP* **05** (2006) 026.
7. F. W. Bopp, R. Engel, and J. Ranft, `arXiv:hep-ph/9803437v1`.
8. R. Engel, J. Ranft, and S. Roesler, *Phys. Rev.* **D52** (1995) 1459.
9. C. Tsallis, *J. Stat. Phys.* **52** (1988) 479.
10. G. Wilk and Z. Wlodarczyk, *Eur. Phys. J.* **A40** (2009) 299.
11. **UA1** Collaboration, C. Albajar et al., *Nucl. Phys.* **B335** (1990) 261.
12. J. Whitmore, *Phys. Rept.* **10** (1974) 273.
13. **Aachen-CERN-Heidelberg-Munich** Collaboration, W. Thome et al., *Nucl. Phys.* **B129** (1977) 365.
14. **UA5** Collaboration, G. J. Alner et al., *Z. Phys.* **C33** (1986) 1.
15. **CDF** Collaboration, F. Abe et al., *Phys. Rev.* **D41** (1990) 2330.
16. **ALICE** Collaboration, K. Aamodt, *Eur. Phys. J.* **C65** (2010) 111.
17. **STAR** Collaboration, B. I. Abelev et al., *Phys. Rev.* **C79** (2009) 034909.
18. **PHOBOS** Collaboration, R. Nouicer et al., *J. Phys.* **G30** (2004) S1133.